

Short Note

Least-squares offset-to-angle for AVA purposes

Claudio Guerra, Alejandro Valenciano and Yaxun Tang

INTRODUCTION

With the increasing use of downward-continuation methods to image complex geology, it became important to obtain prestack migrated images for velocity model updating and, if image quality allows, performing amplitude-versus-angle (AVA) studies to infer rock and fluid characteristics. The prestack images used in these tasks are, in 2D case, function of offset-ray parameter (Clapp, 2005) or reflection angle (ADCIGs) (Sava and Fomel, 2003; Biondi and Symes, 2004). They differ not only on the parameter, but in the moment they are computed with respect to the application of the imaging condition. The earlier is computed before imaging by applying slant stack along the offset axis; the former, after imaging, hence a model-space process, by performing slant-stacking on subsurface-offset gathers computed with an adequate prestack imaging condition (Rickett and Sava, 2002). Besides the velocity model update and AVA analysis, a key importance of the ADCIGs is that in the angle-domain the wave-equation inverse problem can be regularized (Valenciano and Biondi, 2007).

The offset-to-angle is the adjoint of the modeling operator which computes subsurface-offset domain common-image gathers (SODCIGs) from ADCIGs. The offset-to-angle transformation can be carried out both in the physical space (z, h) or in the Fourier space (k_z, k_h) . As we show, in any of these spaces, the offset-to-angle operator is non-unitary implying that the obtained image in the angle domain is a poor estimate of the model. The expression of the differences between the estimate of the model and the "true" model are kinematic artifacts and amplitude variations which bias the AVA response.

As already pointed out by Sava and Biondi (2001), the limited offset and depth wavenumber bandwidths are source of inaccuracies in the offset-to-angle transformation. This, by itself, causes the operator not to be unitary. Moreover, as we shall see, the other source of the non-unitary behavior of the offset-to-angle operator is related to the discretization of the slant-stack integral which can be easily attacked by applying an adequate weighting function to the transformation. Another way to avoid the biased amplitudes is to solve an inverse problem in such a way that the least-squares model is a better approximation of the "true" model. Here, we compute the simple weighting function to be applied along with the non-iterative scheme and formulate the inverse problem, in the physical space, in the least-squares sense. We test both methods and show examples ***** of how different AVA signatures are affected by the fact

that offset-to-angle transformation is non-unitary and how the least-squares approach recover the correct AVA response.

THE OFFSET-TO-ANGLE TRANSFORMATION

The offset-to-angle transformation can be expressed by the integration of the SODCIG, $P(z, h)$, along a certain slanted path, according to the equation

$$Q(z, \gamma) = \int_A \varrho[P(z, h)] dh|_{z=\zeta(\gamma, h)}, \quad (1)$$

where $Q(z, \gamma)$ is the output ADCIG, γ is the aperture angle, h is the subsurface offset, ϱ is the *rho*-filter which aims to yield the correct phase of the output ADCIG (Claerbout, 1997), A is the domain of integration that defines the range of subsurface offsets to be summed, and $\zeta(\gamma, h)$ is the slanted path given by

$$\zeta(\gamma, h) = z_0 + h \tan \gamma, \quad (2)$$

where z_0 is the depth coordinate at zero subsurface offset.

Initially, to investigate the amplitude behavior of the offset-to-angle we start with a synthesized ADCIG with a flat AVA response (Figure 1a). This angle-gather is submitted to a non-weighted angle-to-offset transformation resulting in the SODCIG of Figure 1b. The non-weighted transformation of the SODCIG back to angle (Figure 1c) shows an undesirable amplitude decrease with angle (Figure 1d). Notice the cosine-like shape of the amplitude distribution. This shape can be explained by the fact that, as the reflection angle γ varies, the interval, dh , in which the slant-stacking integral is discretized must varies according to $\frac{dh}{\cos(\gamma)}$. By applying the weight $\frac{1}{\cos(\gamma)}$ to the offset-to-angle transformation the amplitudes are not yet reasonably recovered (Figure 1e and f), because the original SODCIG was computed without weighting the amplitudes. Figure 2a shows the ADCIG corresponding to a offset-to-angle transformation from a SODCIG obtained with a weighted angle-to-offset transformation. Notice on Figure 2a that now the AVA tendency is correctly recovered, except for the limiting angles due to edge effects.

Because of the limited domain of integration in equation 1 and limited bandwidth of the migrated data, the offset-to-angle transformation is non-unitary. Hence, we pose it as a least-squares inverse problem in the next section.

LEAST-SQUARES OFFSET-TO-ANGLE TRANSFORMATION

The regularized least-squares inverse problem of the offset-to-angle transformation can be expressed as the minimization of the objective function

$$\mathbf{J}_r(\mathbf{m}) = \|\mathbf{p} - \mathbf{p}_{\text{obs}}\| + \epsilon \mathbf{m}'\mathbf{m} = \|\mathbf{L}\mathbf{q} - \mathbf{p}_{\text{obs}}\| + \epsilon \mathbf{m}'\mathbf{m}, \quad (3)$$

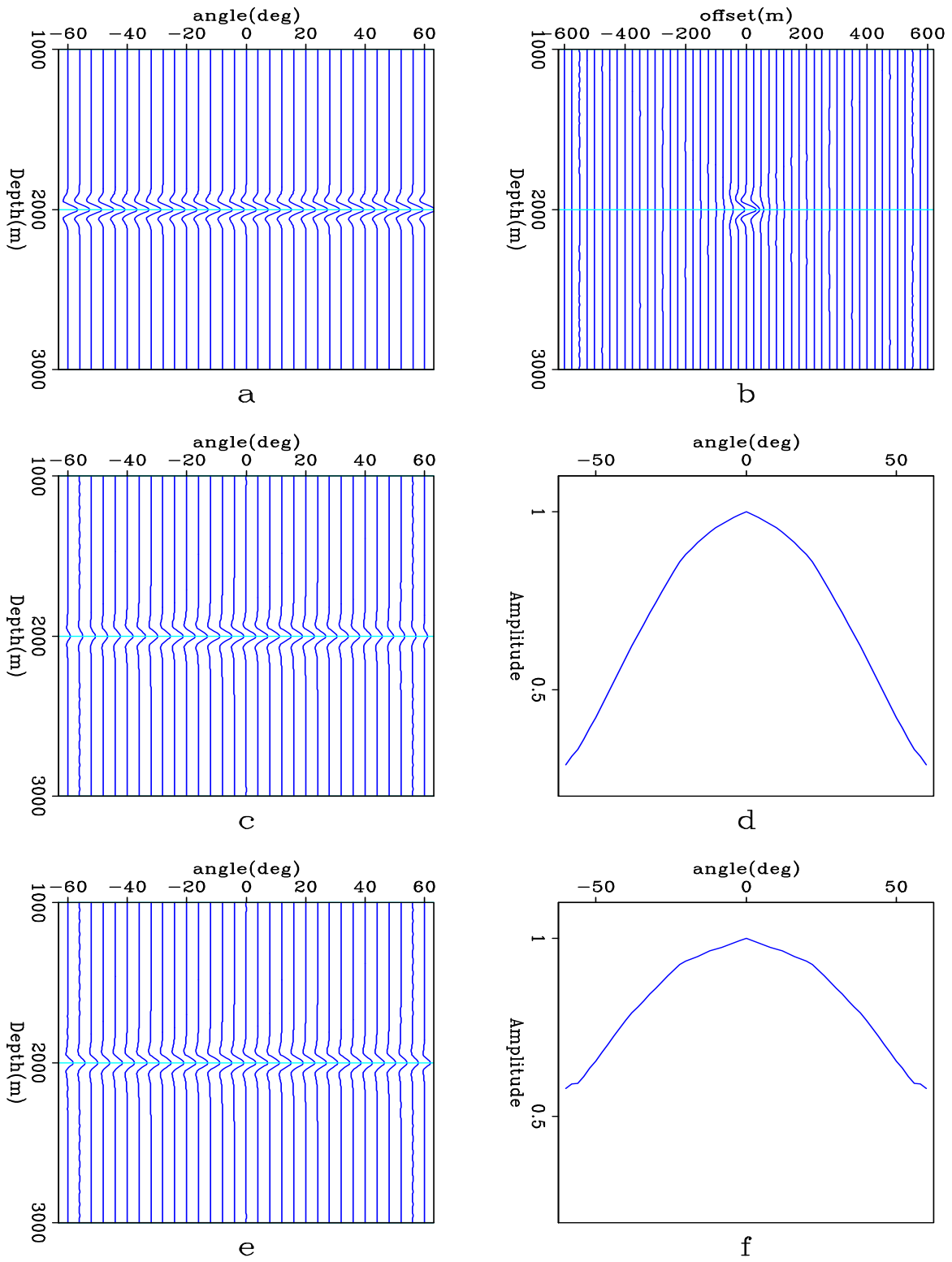
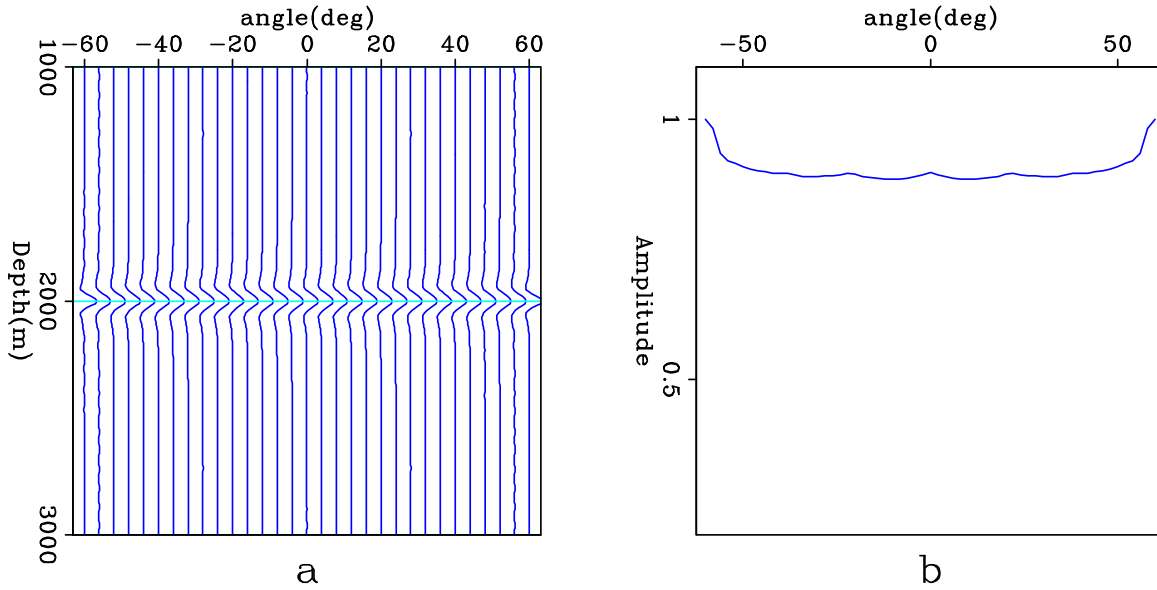


Figure 1: test1 [ER]

Figure 2: `test2` [ER]

where \mathbf{L} corresponds to a modeling operator which models SODCIGs (\mathbf{p}) from ADCIGs (\mathbf{q}) by applying a linear Radon transform. The parameter ϵ is to balance the importance between the two goals. The minimization of $\mathbf{J}_r(\mathbf{m})$ leads to

$$\mathbf{L}\mathbf{q} - \mathbf{p}_{\text{obs}} \approx \mathbf{0} \quad (4)$$

$$\epsilon \mathbf{I}\mathbf{q} \approx \mathbf{0} \quad (5)$$

$$(6)$$

I is the identity operator used here as the regularization operator.

In the next section the examples show the impact of the use of the weighting function and of the least-squares offset-to-angle transformation on the AVA response.

EXAMPLES

We start our analysis with a synthetic ADCIG which shows a reflector with some amplitude variation along the angle axis. The ADCIG is then transformed to subsurface-offset domain by applying on it the $\frac{1}{\cos(\gamma)}$ -weighted modeling operator, yielding a SODCIG which will be transformed back to angle using three different schemes: a) the program OFF2ANG, in the Fourier space, implemented in SEPlib; b) by applying the weighted slant-stack in the physical space; and c) by applying the iterative least-squares inverse strategy. The results of these three transformations are to be compared to the original ADCIG.

According to Castagna et al. (1998) AVA anomalies due to the presence of gas in sand reservoirs embedded in shales can be divided into 4 classes depending on the acoustic-impedance

contrast between these rocks. Particularly, class 3- and class 4-AVA anomalies are characterized by lower acoustic-impedance sand reservoirs. For the first AVA class amplitudes become more negative as reflection angle increases and for the second, less negative. The two following examples are related to these two AVA classes.

Figure 3 stands for the class 3-example. The frames in show the original ADCIG (Figure 3a), the corresponding SODCIG (Figure 3b), the ADCIGs computed with OFF2ANG from SEPlib (Figure 3c), with the weighted slant stack (Figure 3d), and the least-squares offset-to-angle (Figure 3e). Additionally, Figure 3f shows the peak amplitudes, normalized to 1, of the reflector in these three computed ADCIGs (dash for OFF2ANG from SEPlib, dots for the weighted slant stack, and dot-dash for the least-squares solution) and of the original one (continuous line). In spite of the fact that OFF2ANG and weighted slant stack methods give reasonable results, the least-squares offset-to-angle transformation matches almost perfectly the phase response and the amplitudes of the original ADCIG. Both OFF2ANG and weighted slant stack bias the near-angle amplitudes in direction of higher values. In the case of AVA analysis using partial angle-stacks, like near ($0 - 20^\circ$) and far($20 - 40^\circ$), for instance, this amplitude bias should cause a class 3-AVA be under-evaluated.

Figure 4 stands for the class 4-example. All the frames corresponds to the same kind of data shown in Figure 3 for the case of the class 3-AVA. Again, the least-squares offset-to-angle transformation recovers perfectly the phase information and the amplitudes of the original ADCIG. Now, because of the near-angle amplitude biasing, AVA analysis with partial angle-stacks should cause this class 4-AVA be over-evaluated.

In the next example, SODCIGs from shot-profile migration of an acoustic finite-difference synthetic data are transformed to angle domain using the 3 methods previously mentioned. The data consists of split-spread shots, spaced every 10 m, with 1001 receivers 10 m apart, resulting in a maximum source-receiver offset of 5000 m. At 1000 m a plane reflector separates the upper layer with $v_1 = 4000m/s$ from the bottom layer with $v_2 = 3500m/s$. Figure 5 shows an ADCIG computed with OFF2ANG (a), weighted slant stack (b), and least-squares offset-to-angle (c). In Figure 6, the peak amplitudes and the expected AVA are displayed using the same convention as in the previous example. Here we need to make a small digression. The imaging condition in the shot-profile migration is cross-correlation between downgoing and upgoing wavefields. This imaging condition itself is not prone to yield true-amplitude results. Again, the least-squares offset-to-angle transformation yields better results.

CONCLUSIONS

I showed how to estimate angle-domain parameters from the subsurface-offset domain using what I call weighted offset-to-angle, particularly subsurface-offset Hessian diagonals. The proposed approach provides useful information, which can be confirmed by the amplitude compensation results. The transformation of off-diagonal terms of the subsurface-offset Hessian indicates that the results are not strongly dependent on the amplitude distribution in the ADCIGs. However, it is still not clear how to use these transformed off-diagonal terms in inversion schemes.

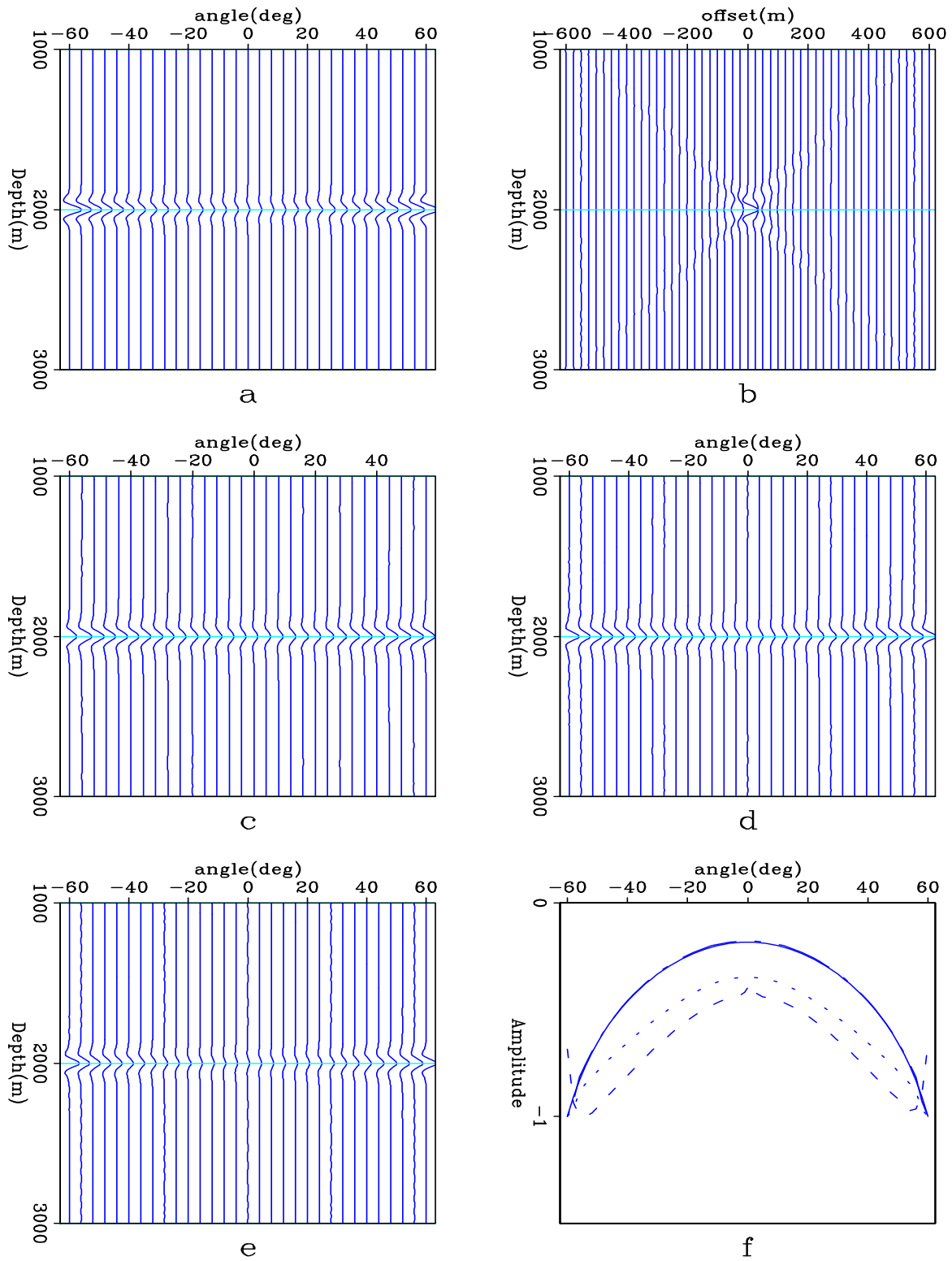


Figure 3: test3 [ER]

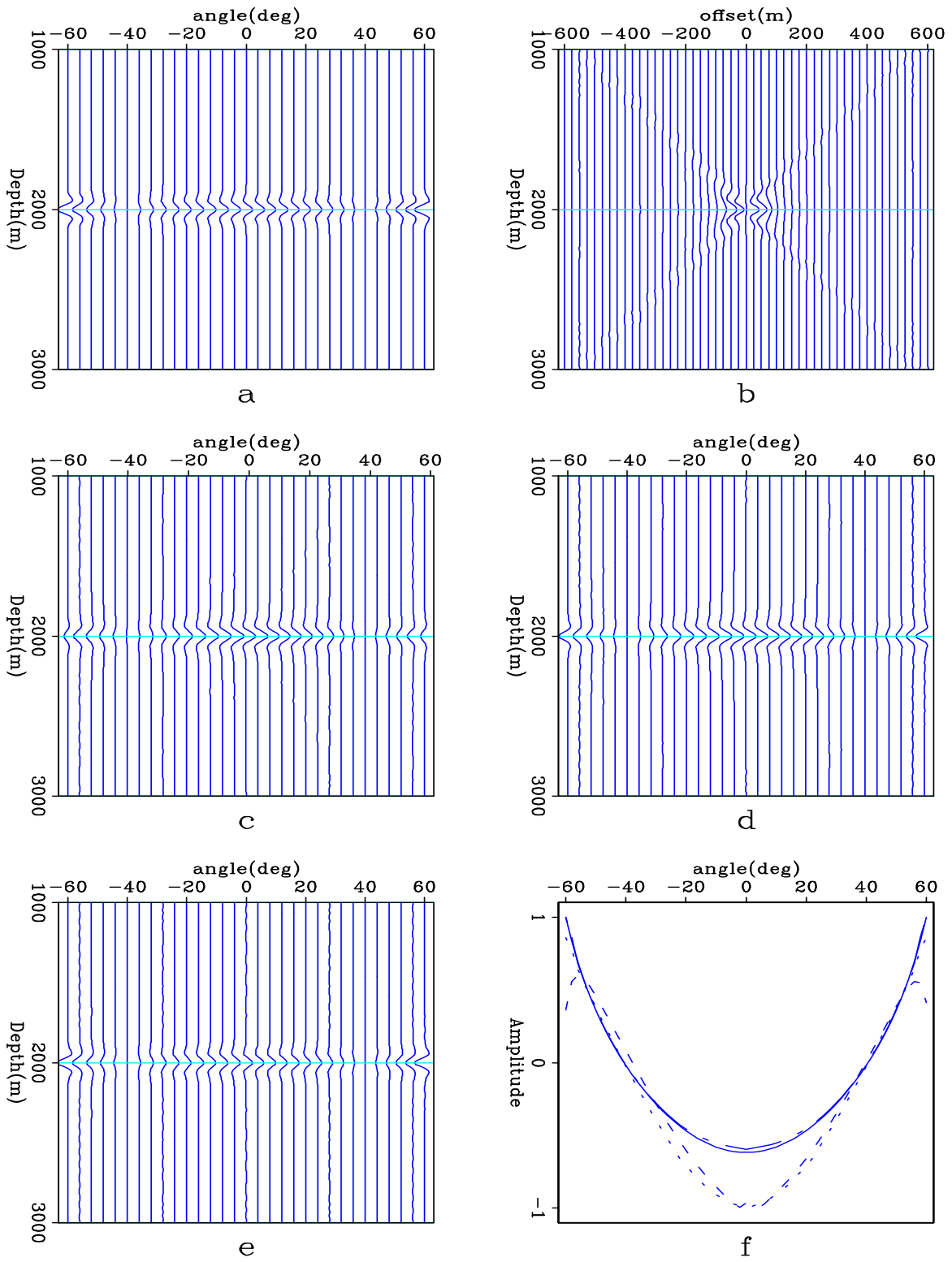


Figure 4: test4 [ER]

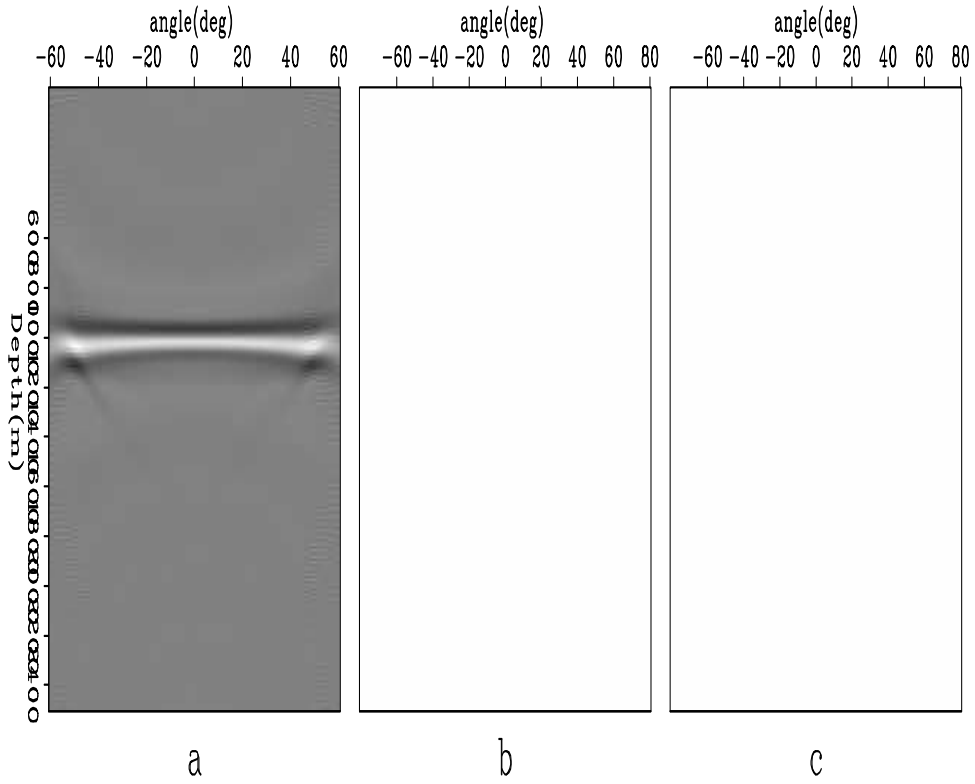


Figure 5: test5 [ER]

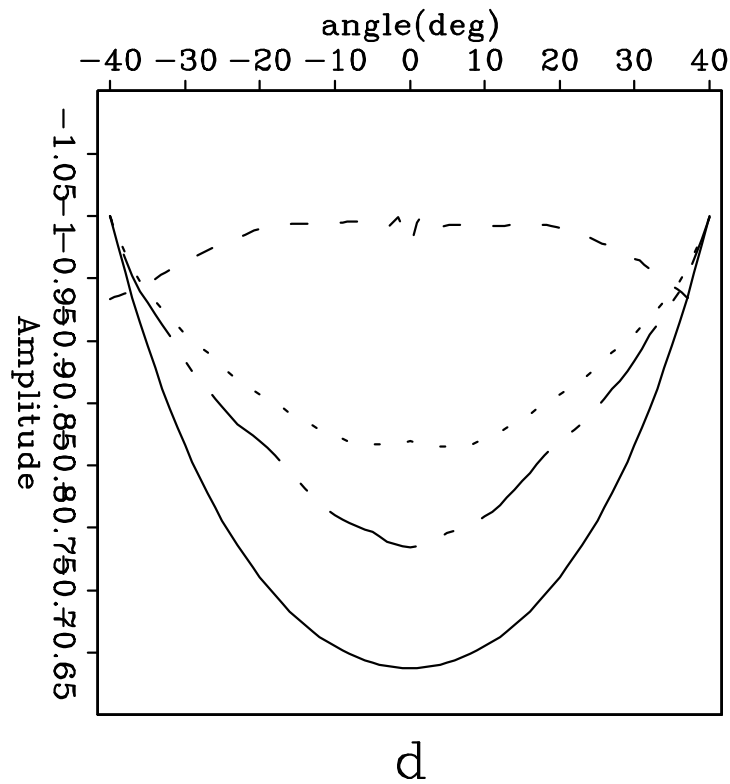


Figure 6: test6 [ER]

ACKNOWLEDGEMENTS

I would like to thank Alejandro Valenciano for providing me the subsurface-offset domain Hessian and common-image gathers and for the explanations and fruitful discussions.

REFERENCES

- Biondi, B. and W. Symes, 2004, Angle-domain common-image gathers for migration velocity analysis by wavefield-continuation imaging: *Geophysics*, **69**, 1283–1298.
- Castagna, J. P., H. W. Swanz, and D. J. Foster, 1998, Framework for avo gradient and intercept interpretation: *Geophysics*, **63**, no. 3, 948–956.
- Claerbout, J., 1997, Imaging the earth's interior: http://sepwww.stanford.edu/sep/prof/toc_html/iei.
- Clapp, M. L., 2005, Imaging under salt: illumination compensation by regularized inversion: Ph.D. thesis, Stanford University.
- Rickett, J. E. and P. C. Sava, 2002, Offset and angle-domain common image-point gathers for shot-profile migration: *Geophysics*, **67**, 883–889.
- Sava, P. and B. Biondi, 2001, Amplitude-preserved wave-equation migration: *SEP*–**108**, 1–26.
- Sava, P. C. and S. Fomel, 2003, Angle-domain common-image gathers by wavefield continuation methods: *Geophysics*, **68**, 1065–1074.
- Valenciano, A. A. and B. Biondi, 2007, Wave-equation inversion prestack hessian: *SEP*-125, pages 201–209.